Ab Initio Kinetics for the Unimolecular Reaction $C_6H_5OH \rightarrow CO + C_5H_6$†

Z. F. Xu and M. C. Lin*

Department of Chemistry, Emory University, Atlanta, Georgia 30322

Received: September 15, 2005; In Final Form: November 10, 2005

The unimolecular decomposition of C_6H_5OH on its singlet-state potential energy surface has been studied at the G2M//B3LYP/6-311G(d,p) level of theory. The result shows that the most favorable reaction channel involves the isomerization and decomposition of phenol via 2,4-cyclohexadienone and other low-lying isomers prior to the fragmentation process, producing *cyclo*-C_5H_6 + CO as major products, supporting the earlier assumption of the important role of the 2,4-cyclohexadienone intermediate. The rate constant predicted by the microcanonical RRKM theory in the temperature range 800−2000 K at 1 Torr − 100 atm of Ar pressure for CO production agrees very well with available experimental data in the temperature range studied. The rate constants for the production of CO and the H atom by O−H dissociation at atmospheric Ar pressure can be represented by $k_{CO} = 8.62 \times 10^{15}\, T^{-0.61} \exp(-37\,300/T)\ s^{-1}$ and $k_H = 1.01 \times 10^{71}\, T^{-15.92} \exp(-62\,800/T)\ s^{-1}$. The latter process is strongly *P*-dependent above 1000 K; its high- and low-pressure limits are given.

1. Introduction

Phenol (C_6H_5OH), a key intermediate in the oxidation of benzene and substituted benzenes, plays an important role in the combustion of those aromatic compounds. Studies on its pyrolysis mechanism have been carried out experimentally in many laboratories. In 1975, Cyprès and Bettens[1] investigated the decomposition of isotopically labeled phenol between 938 and 1138 K at atmospheric pressure. They concluded that the decomposition reaction was initiated by hydroxylic H-migration to an ortho or the para carbon, followed by the decomposition to cyclopentadiene and CO. In 1989, Lovell, Brezinsky, and Glassman[2] studied the pyrolytic reaction at 1 atm between 1064 and 1162 K in a turbulent-flow reactor by analyzing concentration−time profiles of three major decomposition products: carbon monoxide, cyclopentadiene, and benzene. They assumed that the decomposition process was initiated by the dissociation of the C_6H_5O-H bond followed by the fragmentation of C_6H_5O yielding *cyclo*-C_5H_5 + CO; they estimated the rate constant for $C_6H_5OH \rightarrow C_6H_5O + H$ to be $k_{lbg,H} = 2.67 \times 10^{16} \exp(-44\,700/T)\ s^{-1}$. Independently in 1989, Manion and Louw[3] studied the decomposition reaction using a flow reactor in the H_2 carrier gas at atmospheric pressure in a wider temperature range of 922−1175 K. They also considered that the radical mechanism similar to that of Lovell, Brezinsky, and Glassman could reasonably explain the CO produced and gave a rate constant expression: $k_{ml,CO} = 3.31 \times 10^{13} \exp(-36\,000/T)\ s^{-1}$. In 1998, Horn et al.[4] investigated the pyrolysis of phenol at high temperatures using a shock tube from 1450 to 1650 K at ∼2.5 atm Ar pressure. From their time-resolved measurements of both CO and H atoms, they concluded that the dominant initiation reaction is the direct formation of CO after the initial isomerization of phenol. The rate constants for CO and H atom production were deduced to be $k_{hrfj,CO} = 1.0 \times 10^{12} \exp(-30\,600/T)\ s^{-1}$ and $k_{hrfj,H} < 0.15\, k_{hrfj,CO}$.

Theoretically, in 2001, Nguyen and co-workers[5] studied the potential energy surface for the isomerization and decomposition of $C_6H_5OH^+$ at both B3LYP/6-311++G(d,p) and CASPT2/6-31G(d,p) levels of theory. In 2003, Zhu and Bozzelli[6] studied the isomerization and decomposition mechanism of the phenol molecule at the CBS-QB3//B3LYP/6-311G(d,p) level of theory. However, they did not find the pathway leading to the formation of the key decomposition products, *cyclo*-C_5H_6 + CO, as reported experimentally.

In view of the practical importance of phenol to hydrocarbon combustion, we have attempted to characterize the full potential energy surface of the system by carefully mapping out various

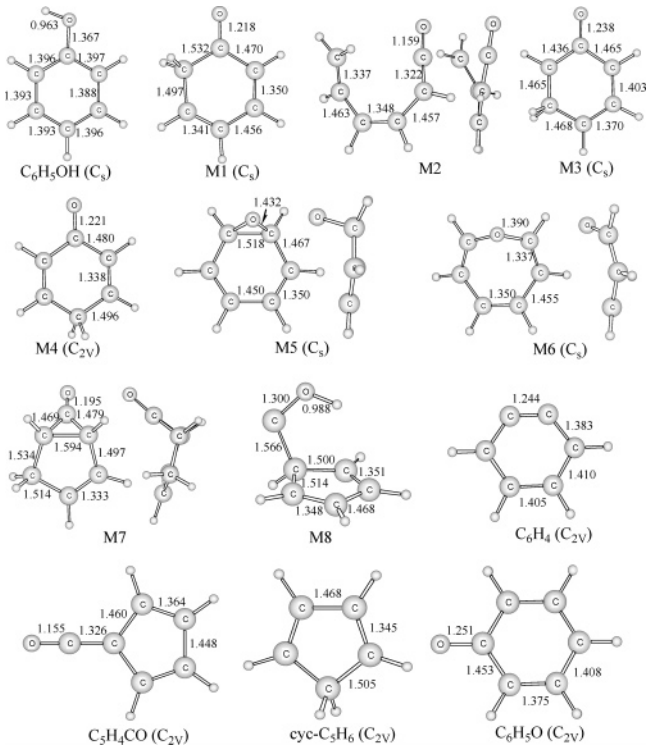

Figure 1. Geometries of the reactants, products, and intermediates (length in Å and angle in deg) optimized at the B3LYP/6-311G(d,p) level of theory.

† Part of the special issue "William Hase Festschrift".

* Corresponding author. M. C. Lin; email address: chemmcl@emory.edu.

10.1021/jp055241d CCC: $33.50
Published on Web 12/30/2005

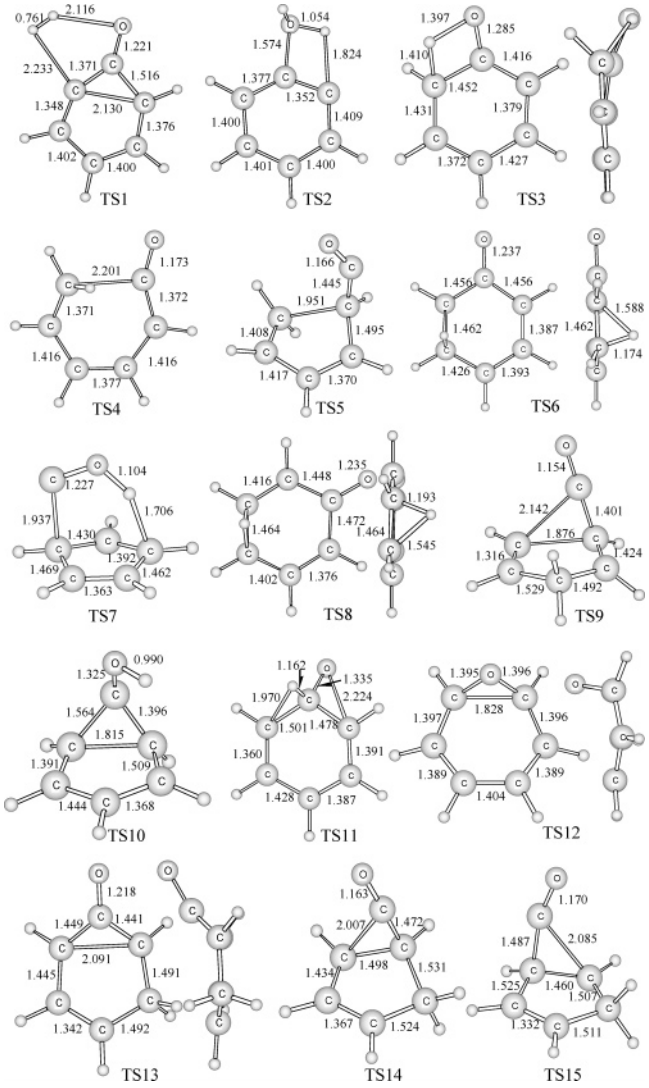

Figure 2. Geometries of the transition states (length in Å and angle in deg) optimized at the B3LYP/6-311G(d,p) level of theory.

possible isomerization and fragmentation processes employing the G2M method.[7] We also predicted the rate constants for the major product channels mentioned above by means of statistical theory analysis for comparison with the reported values. The result is presented in the following sections in detail.

2. Computational Methods

The geometries of the reactants, products, intermediates, and transition states on the singlet electronic ground-state potential energy surface (PES) of the C_6H_5OH decomposition were optimized[8] by the density functional theory at the B3LYP level[9,10] with the 6-311G(d,p) basis set. All the stationary points have been identified for local minima and transition state by vibrational analysis. Unscaled vibrational frequencies were employed for the calculation of zero-point energy (ZPE) corrections, the characterization of stationary points, and rate constant calculations. For a more accurate evaluation of the energetic parameters, higher-level single-point energy calculations of the stationary points were carried out by the modified Gaussian-2 (G2M) theory,[7] based on the optimized geometries at the B3LYP/6-311G(d,p) level of theory. The G2M(CC5) method calculates the base energy at the PMP4/6-311G(d,p) level of theory and improves it with the expanded basis set and coupled cluster corrections as well as a "higher-level correction (HLC)". All electronic structure calculations were performed with the *Gaussian 98* program.[11]

The microcanonical Rice−Ramsperger−Kassel−Marcus (RRKM) theory[12] was employed to calculate the rate constants for the barrierless association reaction by *VARIFLEX*[13] and the *ChemRate* code.[14] The component rates were evaluated at the *E*/*J*-resolved level, and the pressure dependence was treated by one-dimensional master equation calculations using the Boltzmann probability of the complex for the *J*-distribution.

3. Results and Discussion

3.1. Potential Energy Surface and Reaction Mechanism. The geometries of the reactants, products, intermediates, and transition states optimized at the B3LYP/6-311G(d,p) level of theory are shown in Figures 1 and 2. The predicted vibrational frequencies and moments of inertia for all of these species are summarized in Table S1 (Supporting Information) and their *z*-matrices in Table S2 (Supporting Information). The potential energy diagram obtained at the G2M//B3LYP/6-311G(d,p) level of theory is presented in Figure 3. Unless otherwise specified, all the energies cited below were obtained by the G2M method relative to that of the phenol molecule in its ground electronic state.

From Figure 3, one can see that there are three possible direct decomposition product channels

$$C_6H_5OH \rightarrow C_6H_5O + H$$
$$\rightarrow C_5H_4CO + H_2$$
$$\rightarrow C_6H_4 + H_2O$$

The first reaction channel is the hydroxylic H-atom elimination process, which takes place without an intrinsic transition state. The dissociation energy of the C_6H_5O-H bond is predicted to be 89.1 kcal/mol at 0 K. This value compares reasonably with the dissociation energy, 86.6 ± 1.6 kcal/mol, calculated according to the experimental heats of formation of C_6H_5OH, C_6H_5O, and H taken from literature.[15] Our value may be compared with those reported by Blanksby and Ellison[16] and Mulder et al.[17] at 298 K, 90.0 ± 3.0 kcal/mol and 86.7 ± 0.7 kcal/mol, which give rise to the dissociation energy values at 0 K, 88.7 ± 3.0 kcal/mol and 85.4 ± 0.7 kcal/mol, respectively. To describe the kinetics of the dissociation process, $C_6H_5OH \rightarrow C_6H_5O + H$, the minimum-energy path was optimized manually by varying the separation of $C_6H_5O\cdots H$ point by point at an interval of 0.1 Å at the B3LYP/6-311G(d,p) level of theory and scaled with the G2M energy, as shown in Figure 4, which can be approximately represented by the Morse function $V(r) = D_e\{1 - \exp[-4.388(r - 1.08)]\}$, with $D_e = 97.4$ kcal/mol at the G2M level.

The second channel is a concerted dehydrogenation process producing C_5H_4CO (2,4-cyclopentadien-1-ylidene methanone) by the transition state TS1. At TS1, shown in Figure 3, the forming bonds of H−H and C−C are 0.761 Å and 2.130 Å, and the breaking bonds of C−H, O−H, and C−C are 2.223 Å, 2.116 Å, and 1.516 Å, respectively. Although the energy of the products ($C_5H_4CO + H_2$) is only 41.7 kcal/mol higher than that of phenol, this process is uncompetitive because of its exceedingly high potential barrier, 102.1 kcal/mol.

The third channel is a dehydration reaction producing C_6H_4 (benzyne); in the reaction via TS2, one of the ortho-H atoms bends toward the oxygen atom with the O−H separation at 1.054 Å and the breaking C−H and C−O bond lengths at 1.824 Å and 1.574 Å, respectively. The endothermicity of the reaction

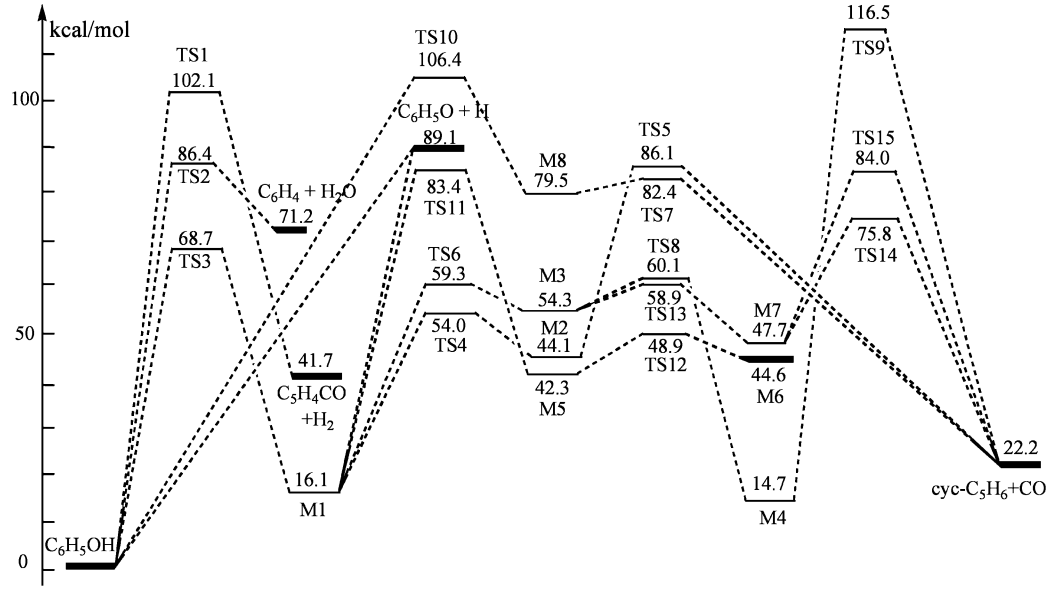

Figure 3. Schematic energy diagram predicted at the G2M//B3LYP/6-311G(d,p) level of theory on the singlet-state potential energy surface. $E(C_6H_5OH, G2M) = -306.920\ 531$ au.

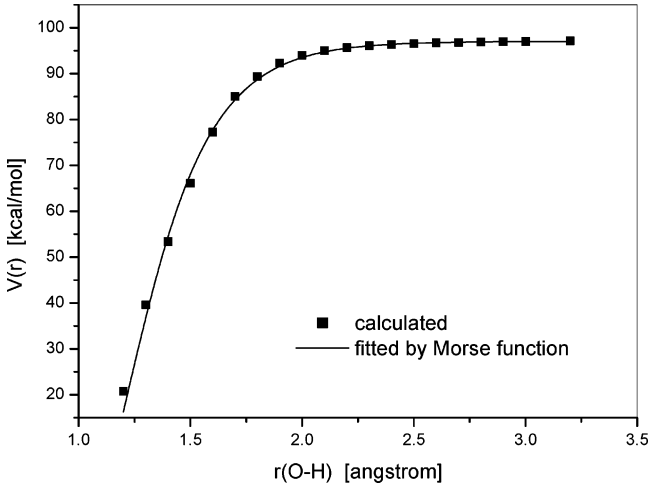

Figure 4. Morse curve for the direct decomposition process, $C_6H_5OH \rightarrow C_6H_5O + H$.

is predicted to be 71.2 kcal/mol, and its potential barrier, 86.4 kcal/mol, is lower than that of the dehydrogenation reaction by 15.7 kcal/mol.

In addition to the above simple direct decomposition channels, there are other more complex isomerization and decomposition processes producing *cyclo*-C_5H_6 + CO and oxepin (M6), as shown in Figure 3. Two isomerization reactions from phenol have been predicted to lead to intermediates M1 (2,4-cyclohexadienone) and M8 (C_5H_5COH, hydroxylpentadienyl methylene) via TS3 and TS10, respectively, in the first step. TS3 represents the transition state for the migration of the hydroxylic H atom to an ortho-C site with the breaking O−H bond length of 1.397 Å and the forming C−H bond length of 1.410 Å; these parameters are the same as those calculated by Zhu and Bozzelli at the B3LYP/6-311G(d,p) level of theory.[6] The potential barrier at TS3 is predicted to be 68.7 kcal/mol, which is 1.0 kcal/mol smaller than Zhu and Bozzelli's value[6] computed by the CBS-QB3 method. TS10 corresponds to the transition state for the two ortho-C atoms moving toward each other with the C−C separation of 1.815 Å forming a five-membered ring, while the breaking C−C bond elongates to 1.564 Å, leading to the formation of the hydroxyl methylene moiety. The barrier of TS10 is predicted to be 106.4 kcal/mol, which is higher than that of TS3 by 37.7 kcal/mol. The energies of M1 and M8 relative to that of phenol are 16.1 and 79.5 kcal/mol, respectively. Although the decomposition from M8 to *cyclo*-C_5H_6 + CO can occur readily, because TS7 is only 2.5 kcal/mol higher than M8, the probability of producing *cyclo*-C_5H_6 + CO by this channel, however, can be neglected because of the high barrier of TS10. In comparison to the above simple, direct decomposition channels, the isomerization/decomposition channel via TS3 to give *cyclo*-C_5H_6 + CO should be the most competitive, as is also reflected by the rate constant predicted for this reaction path, to be discussed later.

In Figure 3, we can see that further reactions from the intermediate M1 (2,4-cyclohexadienone) may include the direct H-atom elimination pathway occurring without an intrinsic transition state and the three isomerization channels via TS4, TS6, and TS11. The first isomerization subchannel produces the isomer M2 (1,3-butadienyl-4-ketene) via TS4; from M1 to TS4, the C−C breaking bond is stretched from 1.532 Å to 2.201 Å and the potential energy of TS4 is predicted to be 54.0 kcal/mol. In comparison to the result calculated by Zhu and Bozzelli,[6] the geometric parameters and the energy of the transition state are different. They predicted the C−C breaking bond length to be 2.038 Å by the B3LYP/6-311G(d,p) method and the barrier for the isomerization process to be 90.8 kcal/mol at the CBS-QB3 level of theory, which is much higher than that for TS4 calculated in this work, 54.0 kcal/mol. The intermediate M2 lies above phenol by 44.1 kcal/mol and can undergo further decomposition to *cyclo*-C_5H_6 and CO via TS5, whose C−C forming bond length is 1.951 Å and C−C breaking bond length is 1.445 Å. Because of its high energy barrier, 86.1 kcal/mol, the decomposition from M2 to *cyclo*-C_5H_6 + CO is rather unlikely to compete effectively with other decomposition channels.

The second isomerization subchannel is from M1 to M3, in which the hydrogen atom migrates from the ortho-C to its neighboring meta-C through the transition state TS6. The energies of TS6 and M3 are higher than that of phenol by 59.3 and 54.3 kcal/mol, respectively. The breaking and forming C−H bond lengths at TS6 are 1.588 Å and 1.174 Å, respectively. Apparently, M3 is an unstable intermediate because of its diradical characteristic. From M3, it is easy to transform to the

TABLE 1: Rotational Moments of Inertia and Harmonic Frequencies of Some Species Calculated at the B3LYP/6-311G(d,p) Level of Theory[a]

species	I_a, I_b, I_c (amu)	frequenies (cm^{-1})
C_6H_5OH	318.1, 688.8, 1006.9	231, 343, 406, 421, 515, 536, 633, 698, 760, 819, 829, 884, 960, 983, 1012, 1043, 1094, 1176, 1190, 1199, 1287, 1349, 1371, 1502, 1530, 1638, 1650, 3146, 3166, 3175, 3189, 3196, 3832
C_6H_5O	326.6, 647.1, 973.8	190, 379, 445, 483, 531, 597, 655, 801, 803, 804, 927, 983, 987, 999, 1008, 1088, 1163, 1164, 1271, 1336, 1419, 1442, 1481, 1545, 1587, 3165, 3171, 3188, 3195, 3198
C_5H_6	212.9, 219.2, 421.0	348, 524, 681, 712, 816, 818, 917, 924, 954, 955, 970, 1012, 1112, 1125, 1130, 1266, 1315, 1397, 1415, 1551, 1638, 3010, 3031, 3186, 3196, 3214, 3221
M1	347.3, 671.7, 1008.2	57, 270, 444, 455, 494, 541, 578, 724, 743, 814, 944, 946, 953, 997, 998, 1026, 1159, 1192, 1193, 1242, 1334, 1398, 1408, 1443, 1608, 1693, 1746, 3014, 3033, 3153, 3158, 3183, 3190
M2	475.9, 764.6, 1184.4	69, 119, 153, 193, 354, 447, 501, 569, 621, 671, 774, 796, 903, 950, 962, 977, 1032, 1091, 1163, 1267, 1330, 1429, 1442, 1467, 1659, 1682, 2200, 3110, 3134, 3141, 3154, 3167, 3222
M3	340.0, 693.6, 1023.0	129, 206, 405, 430, 489, 521, 561, 663, 710, 770, 862, 876, 908, 960, 991, 1024, 1114, 1125, 1162, 1260, 1339, 1354, 1365, 1398, 1466, 1528, 1649, 2949, 2949, 3155, 3181, 3183, 3191
M4	344.5, 675.2, 1009.0	126, 313, 362, 455, 506, 577, 577, 751, 769, 860, 881, 948, 962, 991, 1016, 1030, 1141, 1191, 1204, 1267, 1376, 1413, 1413, 1430, 1658, 1695, 1741, 2985, 2992, 3147, 3148, 3182, 3184
M7	335.8, 712.6, 838.3	144, 213, 393, 516, 543, 667, 688, 755, 769, 870, 902, 936, 951, 985, 1002, 1025, 1059, 1078, 1130, 1181, 1235, 1266, 1326, 1360, 1488, 1661, 1923, 3009, 3039, 3136, 3145, 3182, 3205
TS3	343.8, 641.7, 959.3	*i*2136, 216, 363, 458, 519, 528, 615, 632, 751, 777, 828, 870, 958, 988, 1000, 1004, 1076, 1123, 1172, 1181, 1260, 1369, 1395, 1454, 1525, 1539, 1623, 1795, 3082, 3160, 3170, 3191, 3197
TS4	380.1, 729.1, 1083.0	*i*526, 153, 260, 354, 390, 458, 530, 590, 653, 720, 806, 839, 849, 966, 983, 987, 1027, 1087, 1149, 1227, 1277, 1407, 1430, 1506, 1544, 1617, 2013, 3108, 3118, 3131, 3158, 3182, 3209
TS5	386.4, 791.4, 887.6	*i*689, 88, 129, 312, 418, 487, 549, 612, 665, 738, 797, 814, 934, 960, 992, 1021, 1057, 1075, 1104, 1145, 1220, 1275, 1353, 1436, 1489, 1538, 1986, 3073, 3143, 3156, 3164, 3185, 3193
TS6	328.2, 690.8, 1009.4	*i*831, 139, 383, 431, 452, 518, 590, 650, 702, 799, 807, 876, 937, 978, 993, 1010, 1053, 1151, 1171, 1229, 1260, 1335, 1399, 1431, 1529, 1550, 1678, 2488, 3141, 3157, 3180, 3194, 3213
TS8	330.8, 685.8, 1007.3	*i*904, 133, 375, 437, 478, 521, 586, 637, 715, 786, 802, 884, 937, 971, 980, 1010, 1062, 1147, 1170, 1234, 1262, 1358, 1408, 1470, 1495, 1563, 1692, 2358, 3144, 3161, 3179, 3196, 3216
TS9	392.2, 713.2, 842.8	*i*707, 121, 147, 257, 338, 380, 450, 536, 656, 671, 731, 837, 857, 888, 938, 971, 997, 1028, 1153, 1178, 1213, 1276, 1354, 1366, 1471, 1618, 2118, 2919, 3009, 3011, 3151, 3203, 3210
TS13	320.5, 720.9, 961.9	*i*286, 226, 253, 422, 456, 559, 597, 707, 731, 838, 875, 902, 938, 954, 1007, 1022, 1097, 1135, 1147, 1224, 17316, 1339, 1372, 1410, 1419, 1635, 1780, 2970, 3023, 3139, 3151, 3162, 3201
TS14	370.5, 696.3, 772.8	*i*617, 114, 229, 295, 442, 510, 526, 666, 727, 797, 850, 915, 937, 948, 1006, 1021, 1049, 1111, 1144, 1206, 1243, 1287, 1302, 1389, 1478, 1534, 2033, 2937, 3101, 3112, 3186, 3221, 3262
TS15	365.4, 731.9, 815.9	*i*661, 104, 172, 360, 403, 420, 562, 712, 750, 788, 859, 913, 943, 954, 956, 995, 1077, 1123, 1147, 1238, 1263, 1294, 1314, 1379, 1483, 1655, 1992, 2890, 2967, 3007, 3183, 3219, 3236

[a] Species not included in our rate constant calculations can be found in the Supporting Information; the *z*-matrices of all species are calculated.

stable phenol isomer M4 (2,5-cyclohexadienone), which is energetically only 14.7 kcal/mol higher. The isomerization transition state is TS8, with a 60.1 kcal/mol barrier. The breaking and forming C−H bond lengths at TS8 are 1.193 Å and 1.545 Å, respectively. In Zhu and Bozzelli's work,[6] they found a transition state directly connecting M1 and M4 with a barrier as high as 123.8 kcal/mol by the CBS-QB3 method for the 1,3 H-atom migration process. Our result demonstrates that the two-step mechanism for the isomerization of M1 to M4 is more favorable than their one-step mechanism. In addition, M3 can more readily isomerize to M7 via TS13, which has a barrier of 58.9 kcal/mol, slightly lower than that of TS8. As shown in Figures 1 and 2, at TS13 the two ortho-C atoms approach each other at a separation of 2.091 Å and shortened to 1.594 Å at M7, whose energy is computed to be 47.7 kcal/mol. From Figure 3, one can see that M4 and M7 can both decompose to *cyclo*-C_5H_6 and CO, but because of the very high barrier at TS9 (116.5 kcal/mol), the decomposition of M4 to *cyclo*-C_5H_6 and CO is rather difficult and can be ignored kinetically. The decomposition of M7 to *cyclo*-C_5H_6 and CO can occur by two paths: one via TS14 and the other via TS15, with 75.8 and 84.0 kcal/mol barriers, respectively. Apparently, for the production of *cyclo*-C_5H_6, the channel via TS14 is the most favorable decomposition pathway.

The third isomerization subchannel is from M1 to M5 (benzene oxide) via TS11. From Figure 3, we can see that TS11 lies above phenol by 83.4 kcal/mol, which is much higher than TS4 and TS6. At TS11, the oxygen atom approaches the ortho-C to form a three-membered-ring epoxide, while one of the H atoms attached to the ortho-CH_2 group migrates from the ortho-C to the carbonyl C atom. The C−H breaking bond is 1.970 Å, and the C−H and C−O forming bonds are 1.162 Å

and 2.224 Å, respectively. The M5 isomer is energetically higher than phenol by 42.3 kcal/mol; it is predicted to readily isomerize to M6 (oxepin) via TS12, because the forward and reverse isomerization barriers are only 6.6 and 4.3 kcal/mol, respectively, as shown in Figure 3. The C−C breaking bond length is predicted to be 1.828 Å at TS12, which is elongated by 0.210 Å from that at M5. In view of the high barrier of TS11, the probability for formation of the isomers M5 and M6 should be rather small.

3.2. Rate Constant Calculation. From the above discussion for the decomposition mechanism of phenol from its ground state, one can see that the lowest-energy channel to yield the major products, *cyclo*-C_5H_6 + CO, should be which contains

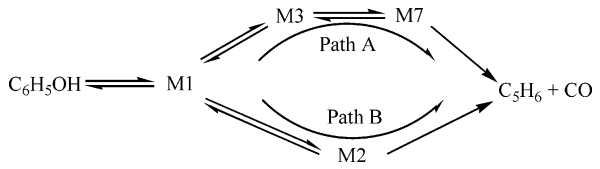

two subchannels: path A and path B. The rate constant for the formation of *cyclo*-C_5H_6 + CO was calculated with the microcanonical RRKM theory by solving a one-dimensional master equation coupling both pathways using the *ChemRate* program[14] in the temperature range 800−2000 K at 1 Torr − 100 atm Ar pressure, including all activation and deactivation processes of the reactant and intermediates, and that for the $C_6H_5OH \rightarrow C_6H_5O + H$ channel was calculated with the microcanonical variational transiton-state theory by *VARIFLEX*[13] for the same condition. The minimum-energy path of $C_6H_5OH \rightarrow C_6H_5O + H$ was described by the above Morse function. In the present study, Lennard-Jones (L-J) parameters taken from the literature[18] are $\sigma = 4.50$ Å and $\epsilon/k_B = 450$ K for C_6H_5OH and its intermediates, and $\sigma = 3.54$ Å and $\epsilon/k_B = 93.3$ K for Ar bath gas for estimating the frequency of collisions. The energy increment was fixed at 10 cm^{-1} in all sum-of-states and density-of-states calculations that were performed using the modified Beyer−Swinehart algorithm.[19] The averaged step size for energy transfer per collision, $\langle \Delta E \rangle_{down}$, was taken to be 200 cm^{-1} for the standard form of the "exponential down" model.[20] The energy bin size, $\Delta E = 100$ cm^{-1}, and a maximum energy limit, $E_{max} = 250$ kcal/mol, were used for the energy integration in the master equation computation to ensure the convergence at high temperature. Rotational moments of inertia and harmonic frequencies of the species included in kinetic calculations are shown in Table 1.

The predicted and experimental rate constants are compared in Figure 5. The solid and dashed lines represent the theoretical rate constants calculated at 1 atm Ar for the formation of CO and H, respectively. The experimental data given by circles and triangles represent the results of Manion and Louw[3] and Horn et al.,[4] respectively. The dotted line indicates the rate constant for the formation of $C_6H_5O + H$ estimated by Lovell et al.[2] In our calculation for k_{CO}, the effect of quantum-mechanical tunneling on the H-migration process from the O atom to the ortho-C at TS3 has been considered (on the basis of the Eckart approach implemented in the *ChemRate* program[14]); the effect on the predicted k_{CO} at 800 K, for example, was found to be less than 5%. The small effect may be attributed in part to the higher kinetically controlling barrier at TS14.

For the production of *cyclo*-C_5H_6 + CO, the predicted rate constant, which was found to be independent of pressure between 1 Torr and 100 atm of Ar in the high-temperature range of 800−2000 K, is in excellent agreement with the two sets of

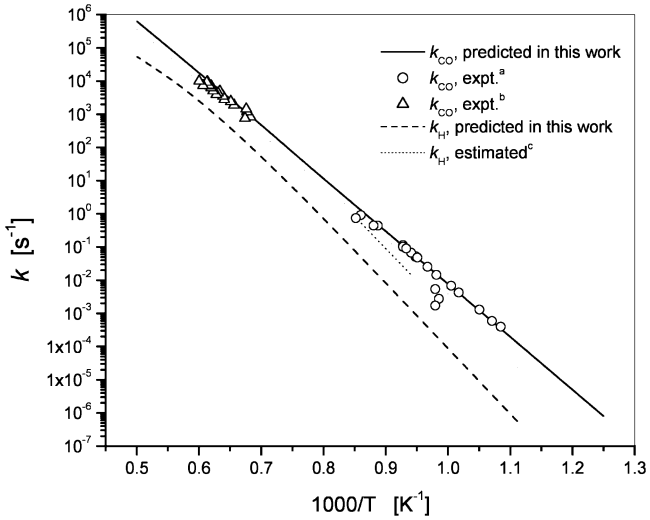

Figure 5. Comparison of the predicted rate constants with the experimental data. [a]ref 3; [b]ref 4; [c]ref 2.

experimental data measured on the basis of CO formation. The dominant pathway is predicted to be path A, whose branching ratios at 1000 and 1500 K are 0.96 and 0.89, respectively. For the production of $C_6H_5O + H$, however, the predicted rate constant is smaller than the estimated value[2] by about 1 order of magnitude. On the other hand, our predicted values for k_{CO} and k_H at 1500−1600 K, giving $k_H/k_{CO} = 0.13-0.14$, are consistent with the estimation of Horn et al., $k_H/k_{CO} < 0.15$. It should be mentioned that the trapping of C_6H_5OH by the two most stable intermediates, M1 and M4, under CO production conditions was found to be insignificant at pressure as high as 100 atm, and the inclusion of the path from M4 to CO + C_5H_6 contributes negligibly to k_{CO} because of the high barrier at TS9.

For practical applications, the rate constants for production of CO and H with Ar as the third body have been fitted to the expressions

$$k_{CO} = 8.62 \times 10^{15}\, T^{-0.61} \exp(-37\,300/T)\ s^{-1}$$

$$k_H^{1atm} = 1.01 \times 10^{71}\, T^{-15.92} \exp(-62\,800/T)\ s^{-1}$$

$$k_H^{\infty} = 3.33 \times 10^{17}\, T^{-0.51} \exp(-46\,100/T)\ s^{-1}$$

$$k_H^0 = 2.56 \times 10^{94}\, T^{-28.21} \exp(-63\,400/T)\ cm^3\ molecule^{-1}\ s^{-1}$$

for the temperature range 800−2000 K. It should be mentioned that, in our calculation for k_H, the contribution of H atoms from the dissociation of 2,4-cyclohexadienone (M1) was neglected in view of the other faster competitive isomerization/decomposition channels. This issue will be addressed in the near future when we investigate the decomposition of chemically activated C_6H_5OH from H + C_6H_5O, for example. In addition, for the production of H atoms, unlike the CO formation process, the rate constant is strongly *P*-dependent above 1000 K. The high- and low-*P* limit rate constants given above can be used for kinetic modeling at high temperatures.

4. Conclusion

The potential energy surface of phenol decomposition has been studied at the G2M//B3LYP/6-311G(d,p) level of theory. The PES and the predicted rate constant show that the most favorable reaction channel to produce C_5H_6 + CO is phenol

isomerization to M1 (2,4-cyclohexadienone) followed by isomerization/decomposition processes involving other low-lying isomers. Our result supports the assumption of Cyprès and Bettens and Horn et al. on the important role of M1 in *cyclo*-C_5H_6 formation.

The rate constants have been predicted by the microcanonical RRKM and/or variational transition-state theories in the temperature range 800−2000 K. The predicted rate constant for CO production agrees very well with available experimental data in the temperature range studied. The predicted result for H-atom production was found to be much smaller than the estimated value by Lovell et al.,[2] although our predicted values for k_{CO} and k_H at 1500−1600 K and 2 atm pressure, giving $k_H/k_{CO} = 0.13-0.14$, are consistent with the estimation of Horn and co-workers,[4] $k_H/k_{CO} < 0.15$, based on direct measurements of CO and H atoms by resonance absorption.

The rate constants for the production of CO and H for the conditions cited above for atmospheric Ar pressure can be represented by

$$k_{CO} = 8.62 \times 10^{15}\, T^{-0.61} \exp(-37\,300/T)\ \mathrm{s}^{-1}$$

$$k_H = 1.01 \times 10^{71}\, T^{-15.92} \exp(-62\,800/T)\ \mathrm{s}^{-1}$$

The CO formation rate constant, unlike that for the H production, is relatively insensitive to pressure due to the coupling of several *P*-dependent forward and reverse processes.

Acknowledgment. The authors are grateful for the support of this work from the Basic Energy Sciences, Department of Energy, under contract no. DE-FG02-97-ER14784. We also thank the Cherry L. Emerson Center of Emory University for the use of its resources, which are in part supported by a National Science Foundation grant (CHE-0079627) and an IBM shared University Research Award. A preliminary calculation by Y. J. Wu on part of PES in 2001 and the useful comments by Dr. I. V. Tokmakov are also appreciated. M.C.L. acknowledges the support from Taiwan National Science Council for a Distinguished Visiting Professorship at the Center for Interdisciplinary Molecular Science, Chiao Tung University, Hsinchu, Taiwan.

Supporting Information Available: Geometries, vibrational frequencies, and moments of inertia of all species. This material is available free of charge via the Internet at http://pubs.acs.org.

References and Notes

(1) Cyprès, R.; Bettens, B. *Tetrahedron* **1974**, *30*, 1253.
(2) Lovell, A. B.; Brezinsky, K.; Glassman, I. *Int. J. Chem. Kinet.* **1989**, *21*, 547.
(3) Manion, J. A.; Louw, R. *J. Phys. Chem.* **1989**, *93*, 3563.
(4) Horn, C.; Roy, K.; Frank, P.; Just, Th. *Symp. (Int.) Combust., [Proc.]* **1998**, 321.
(5) Le, H. T.; Flammang, R.; Gerbaux, P.; Bouchoux, G.; Nguyen, M. T. *J. Phys. Chem. A* **2001**, *105*, 11582.
(6) Zhu, L.; Bozzelli, J. W. *J. Phys. Chem. A* **2003**, *107*, 3696.
(7) Mebel, A. M.; Morokuma, K.; Lin, M. C. *J. Chem. Phys.* **1995**, *103*, 7414.
(8) (a) Gonzalez, C.; Schlegel, H. B. *J. Chem. Phys.* **1989**, *90*, 2154. (b) Gonzalez, C.; Schlegel, H. B. *J. Phys. Chem.* **1990**, *94*, 5523.
(9) (a) Becke, A. D. *J. Chem. Phys.* **1993**, *98*, 5648. (b) Becke, A. D. *J. Chem. Phys.* **1992**, *96*, 2155.
(10) Lee, C.; Yang, W.; Parr, R. G. *Phys. Rev.* **1988**, *37B*, 785.
(11) Frisch, M. J.; Trucks, G. W.; Schlegel, H. B.; Scuseria, G. E.; Robb, M. A.; Cheeseman, J. R.; Zakrzewski, V. G.; Montgomery, J. A., Jr.; Stratmann, R. E.; Burant, J. C.; Dapprich, S.; Millam, J. M.; Daniels, A. D.; Kudin, K. N.; Strain, M. C.; Farkas, O.; Tomasi, J.; Barone, V.; Cossi, M.; Cammi, R.; Mennucci, B.; Pomelli, C.; Adamo, C.; Clifford, S.; Ochterski, J.; Petersson, G. A.; Ayala, P. Y.; Cui, Q.; Morokuma, K.; Malick, D. K.; Rabuck, A. D.; Raghavachari, K.; Foresman, J. B.; Cioslowski, J.; Ortiz, J. V.; Stefanov, B. B.; Liu, G.; Liashenko, A.; Piskorz, P.; Komaromi, I.; Gomperts, R.; Martin, R. L.; Fox, D. J.; Keith, T.; Al-Laham, M. A.; Peng, C. Y.; Nanayakkara, A.; Gonzalez, C.; Challacombe, M.; Gill, P. M. W.; Johnson, B. G.; Chen, W.; Wong, M. W.; Andres, J. L.; Head-Gordon, M.; Replogle, E. S.; Pople, J. A. *Gaussian 98*; Gaussian, Inc.: Pittsburgh, PA, 1998.
(12) Wardlaw, D. M.; Marcus, R. A. *Chem. Phys. Lett.* **1984**, *110*, 230; *J. Chem. Phys.* **1985**, *83*, 3462. Klippenstein, S. J. *J. Chem. Phys.* **1992**, *96*, 367. Klippenstein, S. J.; Marcus, R. A. *J. Chem. Phys.* **1987**, *87*, 3410.
(13) Klippenstein, S. J.; Wagner, A. F.; Dunbar, R. C.; Wardlaw, D. M.; Robertson, S. H. *VARIFLEX*, version 1.00; Argonne National Laboratory, Argonne, IL, 1999.
(14) Mokrushin, V.; Bedanov, V.; Tsang, W.; Zachariah, M.; Knyazev, V. *ChemRate*, version 1.19; NIST: Gaithersburg, MD, 2002.
(15) $\Delta_f H_0°(C_6H_5OH) = -18.5 \pm 0.2$ kcal/mol [Pedley, J. B. *Thermodynamic Data and Stuctures of Organic Compounds*; Thermodynamics Research Center: College Station, TX, 1994; Vol. 1.]. $\Delta_f H_0°(C_6H_5O) = 16.5 \pm 1.4$ kcal/mol [$\Delta_f H_{298}°$ from Tsang, W. Energetics of Organic Free Radicals. In *Energetics and Reactivity in Chemistry Series (SEARCH)*; Simoes, J. A., Greenberg, A., Liebman, J. F., Eds.; Chapman and Hall: London, 1996; and thermal correction from Janoschek, R.; Rossi, M. J. *Int. J. Chem. Kinet.* **2002**, *34*, 550]. $\Delta_f H_0°(H) = 51.6$ kcal/mol [Chase, M. W., Jr.; Davles, C. A.; Downey, J. R., Jr.; Frurip, D. J.; McDonald, R. A.; Syverud, A. N. JANAF Thermochemical Tables. *J. Phys. Chem. Ref. Data* **1985**, *14*, Supplement 1].
(16) Blanksby, S. J.; Ellison, G. B. *Acc. Chem. Res.* **2003**, *36*, 255.
(17) Mulder, P.; Korth, H.-G.; Pratt, D. A.; DiLabio, G. A.; Valgimigli, L.; Pedulli, G. F.; Ingold, K. U. *J. Phys. Chem. A* **2005**, *109*, 2647.
(18) (a) Hippler, H.; Troe, J.; Wendelken, H. J. *J. Chem. Phys.* **1983**, *78*, 6709. (b) Reid, R. C.; Prausnitz, J. M.; Sherwood, T. K. *The Properties of Gases and Liquids*, 3rd ed.; McGraw-Hill: NewYork, 1977. (c) Mourits, F. M.; Rummens, F. H. *Can. J. Chem.* **1977**, *55*, 3007.
(19) Astholz, D. C.; Troe, J.; Wieters, W. *J. Chem. Phys.* **1979**, *70*, 5107.
(20) Rabinovitch, B. S.; Tardy, D. C. *J. Chem. Phys.* **1966**, *45*, 3720.